

# FLACS CFD air quality model performance evaluation with Kit Fox, MUST, Prairie Grass, and EMU observations

Steven R. Hanna<sup>a,\*</sup>, Olav R. Hansen<sup>b</sup>, Seshu Dharmavaram<sup>c</sup>

<sup>a</sup> *Hanna Consultants, 7 Crescent Ave., Kennebunkport, ME, USA*

<sup>b</sup> *GexCon, Bergen, Norway*

<sup>c</sup> *DuPont Company, Wilmington, DE, USA*

Received 4 January 2004; received in revised form 24 May 2004; accepted 24 May 2004

---

## Abstract

The FLACS CFD model, which can be used to estimate the flow and dispersion around buildings and other large roughness obstacles, has been evaluated with tracer data from several field experiments involving obstacle arrays. The following experiments were used in the evaluation exercise: Kit Fox (52 trials with puff and plume releases of slightly dense CO<sub>2</sub> gas in arrays of billboard-shaped obstacles), MUST (37 trials with puff releases of neutrally buoyant tracer gas in an array of 120 shipping containers), Prairie Grass (43 trials with continuous plume releases of neutrally buoyant tracer gas over a flat agricultural field), and the EMU L-shaped building (a wind tunnel experiment involving a release from an open door in the courtyard area of an L-shaped building). The primary focus is on the maximum concentration on the monitoring arcs. The performance statistics are consistently fairly good, with a median of 86% of the predictions within a factor of two of the observations, a median relative bias suggesting a 20% underprediction, a median relative scatter of about 50%, and a median 20% underprediction of the overall experiment maximum. These results are all well within the criteria of acceptance for dispersion models. Evaluations with the EMU L-shaped building data show that 72% of FLACS predictions are within a factor of two of observations, and that the model can predict the dimensions of the recirculating cavity behind the building within a factor of two. It is suggested that these extensive data sets involving tracer releases in obstacle arrays be used to evaluate other CFD models.

© 2004 Elsevier Ltd. All rights reserved.

*Keywords:* CFD model; Model evaluation; Air quality models; Urban dispersion models

---

## 1. Introduction

Air quality models are used to predict the transport and the turbulent dispersion of gases or aerosols after they are released into the atmosphere. Because of advances in computer speed and storage capabilities, it is now practical to apply Computational Fluid Dynamics (CFD) models to some of these air quality modeling scenarios involving short-range dispersion.

The CFD model solves the basic time dependent Navier–Stokes equations, but using a small grid size (of the order 1 m or even less). CFD models are especially useful when the plume is dispersing within arrays of obstacles such as buildings in urban areas or industrial areas, which also can have many pipe racks, tanks, and other types of obstacles. Some CFD models are being run for specific urban building domains with links to urban neighborhood models and further links to mesoscale meteorological models (e.g., Brown et al., 2001). In the past, comprehensive evaluations of CFD models with field observations of tracer dispersion have often been hampered by the slow run times and by

---

\*Corresponding author. Tel.: +207-967-4478; fax: +207-967-5696.

E-mail address: hannaconsult@adelphia.net (S.R. Hanna).

problems with properly maintaining the turbulence (e.g., the experiences with the FEFLO CFD model reported by Hanna et al., 2000). Riddle et al. (2004) and Sklavounos and Rigas (2004) describe recent CFD model applications where comparisons are made with some field data and there are sensitivity studies with turbulence models used by the CFD models.

The current paper concerns the FLACS (FLAME ACCELERATION Simulator) CFD model, which is similar to many other CFD models but which is unique in its use of a distributed porosity approach for parameterizing buildings and other obstacles. The porosity of a grid is represented as a fractional coverage of each grid volume and each grid face with sub-grid obstacles. Turbulence production terms are parameterized for sub-grid objects (Arntzen, 1998). In the current paper, FLACS is evaluated with extensive field observations involving tracer gas releases in three independent field experiments (Kit Fox, MUST, and Prairie Grass) and wind tunnel data from an L-shaped building. The numbers of experimental trials used in the FLACS evaluations are much larger than the numbers used in any prior evaluations with atmospheric tracer data (e.g., the evaluations reported by Riddle et al., 2004).

## 2. Description of FLACS flow and dispersion model

A description of the field experiments and the results of the model evaluation exercise are given in Section 4. First, in the current section, the characteristics of the FLACS CFD model and some justifications for its assumptions are given. FLACS was developed in the early 1980s to simulate the initial dispersion of gas leaks and subsequent explosions in offshore oil and gas production platforms. The conservation equations for mass, momentum, and enthalpy, in addition to conservation equations for concentration and for flammable gas effects, are solved on a Cartesian grid using a finite volume method. The equations are closed using the  $k-\epsilon$  equations for turbulence, as described by Harlow and Nakayama (1967). The SIMPLE pressure correction method (Patankar, 1980) is applied, and extended for compressible flows with source terms for the compression work in the enthalpy equation. Hjertager (1985, 1986) describes the basic equations used in the FLACS model, and Hjertager (1988a,b) present the results of several laboratory and field experiments used in the development of FLACS.

Because accidental explosions around oil platforms are normally preceded by the release and subsequent dispersion of flammable materials in the atmosphere in and around the platform, the FLACS CFD model contains algorithms for calculating the initial dispersion of flammable gas. The use of CFD models to calculate dispersion is widespread in explosion quantitative risk

assessments (Hansen et al., 1999a, 2001), and is required by industry standards in certain countries (NORSOK, 2001). For the land-based chemical process industries, FLACS is used to assist in siting control rooms so they are less likely to be affected by any nearby explosions (van Wingerden et al., 1999).

Since small details of the obstacles on an oil platform can have a significant impact on flame acceleration, the proper representation of the obstacles was a key aspect of the development of the FLACS explosion prediction code. A so-called distributed porosity concept was developed, as a compromise between the need to characterize the geometric details and the need to have the code run in a reasonable time. Obstacles such as structures and pipes are represented as area porosities (the opposite of blockages) on control volume (CV) faces, and are represented as volume porosities in the interior of the CV. Each CV surface or each CV volume is either fully open, fully blocked or partly blocked. For the partly blocked surfaces or volumes, the porosity is defined as the fraction of the area/volume that is available for fluid flow. The resulting porosity model is used to calculate the flow resistance terms, the turbulence source terms from small objects, and the flame speed enhancement due to flame folding in the sub-grid wake. The flame folding parameter is very important for explosion calculations, but irrelevant for pure dispersion calculations. There are several problems that had to be resolved when the porosity methodology was developed. For example, it is desired that the porosity calculations should be automatic within the code, and should not overly influence the results when the grids are translated or their size and shape are changed. It is necessary that closed surfaces or corners should remain closed with different assumed grids, and openings in walls should not depend on the assumed grid. Sub-grid objects (with sizes less than the grid size) must be handled differently than on-grid objects (with sizes greater than the grid size), and special care is needed if more than one sub-grid object is within the same CV. In FLACS, different drag coefficients are used for cylindrical and rectangular sub-grid objects, and significant drag and turbulence are generated only behind an object, and not along an object that partly blocks a CV. To handle all of these conditions within the porosity algorithm in FLACS, ten coefficients are calculated for each control volume. A comprehensive description of this concept is given in Hjertager (1985, 1986) and Arntzen (1998).

For the flow scenarios described in this article, an important consideration is the drag formulation from the partly porous objects and the modeled turbulence production behind objects classified as sub-grid. For the smallest objects, the flow kinetic energy lost due to the drag is directly added as a production term for turbulent energy. With increased size of the sub-grid object relative to the grid size, the sub-grid turbulence

production is gradually decreased. Objects with a dimension of 1.5–2.0 CVs (where the exact limit depends on position on grid) in both cross-flow directions are defined to be on-grid objects. For these objects, there is no sub-grid turbulence production, since the shear layers handle the turbulent production.

Modifications to the standard  $k-\varepsilon$  model have been implemented in FLACS, as briefly listed below:

- For objects with width equal to about one control volume (CV), typical numerical schemes will estimate zero turbulence production, as the  $du/dy$  terms behind the objects will be identical and opposite and will cancel. This situation has been improved by a modification of the discretization for production of turbulent energy.
- Wall functions with no slip condition are implemented for solid surfaces. Analytical models estimate the total production of turbulent energy across the boundary layer, and add production terms to the relevant CVs across the boundary layer, even if the first grid cell is larger than the boundary layer.
- Source terms for the production of turbulent energy due to Rayleigh–Taylor instabilities (when buoyant gas is accelerating denser gas due to gravity) have been included.

Except for these modifications, the  $k-\varepsilon$  model with standard constants is applied in the turbulence model.

During the course of more than 20 years of development and evaluation of the FLACS software, the numerical methods have been steadily modified and revised user guides have had to be developed. Of course this is the case for any code that is in wide use over many years. Currently FLACS uses a second order central difference scheme for the diffusive fluxes, and a second order so-called kappa scheme for the convective fluxes. The kappa scheme is a hybrid scheme, which does a weighting between second order central and upwind difference schemes. Second order schemes in time have also been implemented but are not applied in the default version of FLACS applied in this paper. The second order terms in time are not required for the short time steps used in the current study, and tend to become unstable when the time steps become large.

A pressure correction method is applied in order to obtain a solution that converges. Iterations are repeated until a mass residual of less than  $10^{-4}$  is obtained.

For the calculations of transport and dispersion of gases or small particles, the boundary conditions are usually either (1) no slip solid surfaces, (2) wind inflow (or outflow), or (3) a passive outflow condition at ambient pressure. Prior to the evaluation exercise presented in this paper, the assumed atmospheric boundary layer turbulence inputs have been modified to account for the effects of stability and for the effects of relatively low-frequency lateral meandering flow.

Previously, a logarithmic stationary wind profile with a specific turbulence intensity and length scale could be specified. This would typically lead to an over-prediction of the hazard distance (i.e., an over-prediction of concentrations) from a gas release, because the simulated atmospheric boundary layer turbulence was underestimated. Hanna et al. (2002) and Riddle et al. (2004) report similar results (i.e., underestimation of turbulence) with other CFD models. Using a method suggested by Arya (2001) and Han et al. (2000), FLACS was modified to estimate the turbulent kinetic energy and dissipation rate based on input of Pasquill stability class (from unstable A to stable F) or input of Monin–Obukhov length  $L$ .

In the case of the arrays of obstacles placed on in relatively flat rural surroundings, such as the MUST and Kit Fox and EMU experiments studied in the current paper, the surface roughness length,  $z_0$ , used for the wind inflow boundary condition is based on the assumed roughness upstream of the experiment. For the unstable Pasquill classes (A–C) an average heat flux from the ground (from Arya, 2001) is specified as an input, and is used to calculate the upstream turbulence profiles.

It would be useful to account for the fact that the wind speed and direction in the atmospheric boundary layer vary with time and space over a continuous spectrum. Typical turbulence parameterizations in CFD models are primarily based on engineering approximations of sub-grid turbulence and may not be able to represent atmospheric eddies (fluctuations) with periods of 10–100 s or more (the larger periods are associated with the so-called meandering flow field). If a CFD model does not satisfactorily account for the larger range of atmospheric eddies, it may therefore under-predict turbulence levels and consequently over-predict hazard distances. To better approximate the wide range of atmospheric eddy sizes in the version of FLACS used here, preliminary approximations of larger eddies with periods from 10 to 100 s have been implemented. The periods of the fluctuations could have covered a broader range, but it is assumed that it is sufficient to use two representative periods in the middle of the spectrum. It is anticipated that these approximations can be improved as more experience is gained. In the current method, two harmonic waves with periods 10–15 s (slightly different for the three directions to avoid repetition) and 60–70 s (only for the two horizontal directions and also slightly different to avoid repetition) have been chosen to approximate the meandering flow. Based on standard assumptions in Arya (2001), the total magnitude of these velocity fluctuations is 2.4, 1.9 and 1.3 times the friction velocity,  $u^*$ , in the along wind, cross wind, and vertical directions, respectively. Fluctuations are thus proportional to the wind speed and depend on the surface roughness. Future research will address the sensitivity of the results to these choices and perhaps improve the

methodology. Eddies with periods much longer than 60 s would be of less interest for the CFD scenarios in this paper because of the size of the domain (about 100 to 1000 m) and the duration of the simulation period (about 10–20 min). As stated earlier, in practice, slightly different frequencies are chosen for fluctuations along wind, across wind and vertically to avoid repeated flow patterns. These assumptions represent the default field, which was used for all the simulations reported. It is also possible for the user to arbitrarily specify fluctuations with two sine waves with specified periods and magnitudes in the three directions.

The gas explosion modules in FLACS have been evaluated with data from hundreds of gas explosion experiments in the laboratory and in the field (Hansen et al., 1999b). Previous evaluation exercises involving the dispersion algorithms in FLACS have focused on the dispersion of flammable natural gas, with observed concentrations in the flammable range from 5 to 15%. It was concluded from those studies that the diameter of the cloud after expansion to ambient pressure must be resolved by at least 1 CV to obtain good results. For the Kit Fox and EMU data evaluated later in this paper, these guidelines could be followed, since the initial diameter of the release was 1.5 m for Kit Fox and 4 m for EMU. However, for the MUST and Prairie Grass field data, also evaluated later, the small initial diameters (about 1 cm) and the relatively large domains (about 100–1000 m) made it more difficult to follow this guidance, and much coarser grids than normally used were applied to ensure acceptable simulation times. Consequently, we have to accept the fact that the gas in the CVs near the source will be too dilute. A concept for local grid refinement near the source has been developed (Gjesdal, 2000), but problems with stability limits the use of these algorithms.

The question can be asked, if the FLACS system relies on high-resolution (e.g., 1 m resolution) geometric data to calculate the porosity values, will there be problems in urban areas because the data for large numbers of buildings are not sufficiently detailed? For a small number of buildings it is more likely that detailed CAD data are available. Several organizations are currently sponsoring development of 1 m resolution geometry data for larger cities. However, it is important to note that FLACS can use whatever data are available to approximate the porosity using empirical assumptions. For studies with FLACS of onshore and offshore chemical process facilities, the distribution of pipe lengths and diameters can be specified as much as possible based on the CAD model. However, if for instance, data on the 2" piping in the facility is lacking, an expected amount of 2" piping is added to make the model realistic (this is called the artificial congestion concept). This method was used in the MUST runs described later, where sagebrush (0.40 m tall and shaped

like wide porous boxes near the ground) was added to the domain. It was found that the small sagebrush obstacles did not significantly influence the results, since the MUST obstacles were much larger (about 2.5 m tall and 2.4 m wide and 12.2 m long) and there were 120 of them. To conclude, if details are lacking on the geometry, and if there is known to be a systematic pattern in what is lacking, it is usually not a problem to represent these details approximately (e.g., trees in a park may be represented quickly by assuming a typical shape, density and porosity).

Questions also arise whether the  $k-\epsilon$  model is the most appropriate closure model. A set of (empirical) constants is needed for the  $k-\epsilon$  and for any other turbulence model. The advantage of the  $k-\epsilon$  model is that there is a limited number of equations (two) and constants. Improvements to the model to make it more suitable for transient scenarios have been made, and numerical problems have been corrected where, in the Prairie Grass, Kit Fox, and MUST runs, little turbulence was generated behind an object with size equal to about one grid size. As seen by other modelers (e.g., Riddle et al., 2004) who have applied  $k-\epsilon$  closure to atmospheric dispersion scenarios, too much dissipation of turbulence was observed for scenarios with no buildings or other obstacles (e.g., the Prairie Grass experiment). For urban areas and building obstacles represented by the MUST and Kit Fox scenarios, the regular patterns of obstacles ensured sufficient production of turbulent kinetic energy, as parameterized by the sub-grid concept in FLACS. The weakness of the  $k-\epsilon$  closure method for scenarios large numbers of obstacles is less important. If another alternate turbulent closure model were used, such as a Reynolds stress model, more equations would be needed (at least six) and many more (less well-established) constants are required.

As for all numerical models, the run times for FLACS are roughly proportional to the number of grid cells times the number of seconds simulated times the number of time steps each second. The grids have been made relatively coarse in the current study, as the goal was to obtain relatively quick results. Within a few days, 40 or 50 tracer release trials in a field experiment could be simulated, with about ten 1 GHz Pentium 3 PCs available. The number of time steps each second depends on the time step criteria (i.e. the CFL number), the finest grid size, and the wind speed. If the grid is refined locally, then shorter time steps may be needed to satisfy the CFL criteria. Examples of numbers of CVs and simulation times for the FLACS runs carried out in the current paper are: For Kit Fox (assuming the coarse grid used for this paper), where there are 33,000 CVs, and 300–900 s of simulated time, the typical elapsed time on the PC for one run is two to three hours, but as large as nine hours for one of the experiment trials. For the quality check runs for Kit Fox (assuming a finer grid)

where there are 308,000 CVs, and 350–600 s of simulated time, the typical elapsed time on the PC for four runs is 30, 50, 54 and 150 h. For MUST, where the grid used for calculations contained 55,000–75,000 CVs and where there was 500 s of simulated time, the typical elapsed time on the PC for one run is 6–10 h (one case 15 h). For Prairie Grass, where the grid contained about 50,000 CVs, and where there were 1000–1200 s of simulated time, the typical elapsed time on the PC for one run is about 9–40 h, with the longer simulation times for stability classes A–C (i.e., unstable conditions).

The initialization of the wind field consumes a relatively small amount of time (about 10–50 s). The assumed initial wind field has a logarithmic mean wind profile at the upwind boundary, and subgrid plus larger turbulence components, as described earlier. Then, due to the generation of flows and turbulence by the presence of the obstacles, typically about 10–30 s are needed for the flow to adjust around the obstacles. The presence of buildings will not significantly increase the requirement for simulation time for a given grid, because of the efficiencies offered by the sub-grid porosity assumption.

Although the field experiments studied in the current paper all involve tracer gases, FLACS is also able to model aerosols based on the Eulerian transport equations. The aerosol models have been used to simulate the effect of water sprays on gas dispersion (Hansen, 2003).

### 3. Description of statistical model performance evaluation methods

The FLACS model is evaluated following the approaches for model performance measures for air quality models suggested by Weil et al. (1992), Hanna et al. (1993), and ASTM (2000). This section describes the specific approach used in the current paper, based on a methodology suggested by Hanna et al. (1993) and summarized by Chang and Hanna (2004).

The Kit Fox (Hanna and Chang, 2001), MUST (Biltoft, 2001), and Prairie Grass (Barad, 1958) field experiments used in the current paper all involve tracer samplers or monitors installed on arcs at specific downwind distances (four or five distances are used in these three field experiments). The evaluations in this paper focus on the maximum concentration observed and predicted on a given arc during a given experimental trial. Note that the location of the monitor with the observed maximum is not necessarily the same as the location of the monitor with the predicted maximum. For the EMU L-shaped building (Hall, 1997), where there are not well-defined monitoring arcs, the evaluations focus on observed and predicted concentrations, paired in space and time at several monitor locations.

The use of maximum concentrations on arcs for the model evaluation exercise is fairly standard for evaluations of dispersion models and field experiments in open terrain. Even though the Kit Fox and MUST experiments involve obstacle arrays and tracer releases at heights less than the obstacle heights, the monitoring arcs were set up at distances beyond a few rows of obstacles. Consequently, for those experiments, the flow and dispersion around individual obstacles is not being investigated, and it is felt that the arc-maximum concentrations are appropriate for evaluation. However, the main use of a CFD model, and where it has advantages over more standard models such as Gaussian plume models or Lagrangian puff models, is to provide detailed three-dimensional, time dependent information in the area near (within one obstacle height) of the obstacle. The EMU L-shaped building (observed in a wind tunnel) is the only data set in the current exercise that provides sufficient detail in the area near the building. Future evaluations of CFD models should focus more on the identification of important model outputs and development of methods to evaluate CFD models near obstacles.

The following equations define the statistical performance measures, which include the fractional bias (FB), the geometric mean bias (MG), the normalized mean square error (NMSE), the geometric variance (VG), and the fraction of predictions within a factor of two of observations (FAC2):

$$FB = \frac{(\bar{C}_o - \bar{C}_p)}{0.5(\bar{C}_o + \bar{C}_p)}, \quad (1)$$

$$MG = \exp(\overline{\ln C_o} - \overline{\ln C_p}), \quad (2)$$

$$NMSE = \frac{\overline{(C_o - C_p)^2}}{\bar{C}_o \bar{C}_p}, \quad (3)$$

$$VG = \exp\left[\overline{(\ln C_o - \ln C_p)^2}\right], \quad (4)$$

$$FAC2 = \text{fraction of data that satisfy } 0.5 \leq \frac{C_p}{C_o} \leq 2.0, \quad (5)$$

where

$C_p$ : model predictions of concentration,  
 $C_o$ : observations of concentration,  
 overbar ( $\bar{C}$ ): average over the data set, and  
 $\sigma_C$ : standard deviation over the data set.

A perfect model would have MG, VG, and FAC2=1.0; and FB and NMSE=0.0. Of course, because of the influence of random atmospheric processes, there is no such thing as a perfect model in air quality modeling. In addition to the standard

performance measures defined above, which use data from a large number of experimental trials, the simple ratio of the overall maximum observed concentration to the overall maximum predicted concentration on each arc is listed for each field experiment. Thus, for the 100 m arc of the Prairie Grass field experiment, and over all 43 experimental trials, there is a single overall maximum observed concentration and a single overall maximum predicted concentration. These two maxima may occur during different experiment trials.

All five performance measures defined above should be calculated and considered together, since each measure has pros and cons. For example, the linear measures FB and NMSE can be overly influenced by infrequently occurring high observed and/or predicted concentrations, whereas the logarithmic measures MG and VG may provide a more balanced treatment of extreme high values.

To help interpret the performance measures, the following examples of typical values may be useful: For the fractional bias,  $FB = 0.67$  implies a factor of two mean under-prediction, and  $FB = -0.67$  implies a factor of two mean over-prediction. The geometric mean, MG, can be thought of as the ratio of the geometric mean of  $C_o$  to the geometric mean of  $C_p$ . Consequently, a factor of two mean bias would imply that  $MG = 0.5$  or  $2.0$ , and a factor of four mean bias would imply that  $MG = 0.25$  or  $4.0$ . To interpret the normalized mean square error, NMSE, assume that the mean of the observed concentrations equals the mean of the predicted concentrations. Then  $NMSE = 1$  if the typical error equals the mean and  $NMSE = 4$  if the typical error equals two times the mean. As NMSE becomes much larger than 1.0, it can be inferred that the distribution is not normal but is closer to log-normal (e.g., many low values and a few large values). The geometric variance, VG, expresses the scatter of a log-normal distribution, which can be expressed as, say, “plus or minus 20%”, or “plus or minus a factor of 10”. For example, a factor of 2 scatter would imply  $VG = 1.6$ , a factor of 4 scatter would imply  $VG = 6.8$ , and a factor of 5 scatter would imply  $VG = 12$ .

For models where the relative bias and scatter is small, there are further approximations that can be derived. For example, if  $\bar{C}_o - \bar{C}_p < 0.1$ , then FB equals  $(\bar{C}_o - \bar{C}_p)/\bar{C}_o$ , which can be thought of as the relative under- or over-prediction. That is, a 2% over-prediction leads to  $FB = -0.02$ . Similarly, for small  $(\bar{C}_o - \bar{C}_p)/\bar{C}_o$ , then  $MG = 1 + (\bar{C}_o - \bar{C}_p)/\bar{C}_o = 1 + FB$ . The performance measures for relative scatter, NMSE and VG, also have simple approximations for small  $(\bar{C}_o - \bar{C}_p)/\bar{C}_o$ . For example, since  $(NMSE)^{1/2}$  can be interpreted as the relative scatter, then  $VG = 1 + NMSE$ . These approximations are valid only for small  $(\bar{C}_o - \bar{C}_p)/\bar{C}_o$ . However, since  $(\bar{C}_o - \bar{C}_p)/\bar{C}_o$  is small for many of the FLACS evaluations, it will be seen that these approximations are roughly valid.

Typical magnitudes of the above performance measures and estimates of model acceptance criteria have been summarized by Chang and Hanna (2004) based on extensive experience with evaluating many models with many field data sets. It was concluded that, for research-grade field experiments such as those investigated in this paper, “acceptable” performing models have the following typical performance measures. The fraction of predictions within a factor of two of observations is about 50% (i.e.,  $FAC2 > 0.5$ ). The mean bias is within  $\pm 30\%$  of the mean (i.e.,  $-0.3 < FB < 0.3$  or  $0.7 < MG < 1.3$ ). The random scatter is about a factor of two of the mean (i.e.,  $NMSE < 4$  or  $VG < 1.6$ ). However, these are not firm guidelines and it is necessary to consider all performance measures in making a decision concerning model acceptance. Since most of these criteria are based on research grade field experiments, model performance would be expected to deteriorate as the quality of the inputs decreases.

#### 4. Description of data sets and results of evaluations

In order to demonstrate that a model is performing satisfactorily, it is best to evaluate the model using several independent field experiments. Because the FLACS CFD model is intended for use at industrial sites and urban sites with numerous obstacles, such as buildings, storage tanks, and pipe racks, the focus should be on field experiments involving obstacles. For this reason, the Kit Fox (Hanna and Chang, 2001) and MUST (Biltoft, 2001) experiments were chosen. Also, because of concerns about CFD models’ abilities to maintain the proper atmospheric turbulence levels over an open field in the absence of buildings, the well-known Prairie Grass field experiment (Barad, 1958) is used as part of our evaluations. Finally, to demonstrate the FLACS model’s capabilities to simulate the flow and dispersion patterns at close distances from a single building, the EMU L-shaped building wind tunnel data set (Hall, 1997) is used. The characteristics of these field experiments are summarized below and the results of the statistical evaluations are given.

##### 4.1. Must field experiment

The mock urban setting test (MUST) field experiment consisted of 37 releases of propylene tracer gas in an array of 120 obstacles at the Dugway Proving Ground desert site (Biltoft, 2001). The obstacles were shipping containers, which are about the size of the trailer in a tractor-trailer rig (12.2 m long by 2.42 m wide by 2.54 m high). Fig. 1 shows the arrangement of the array of obstacles as simulated by FLACS. The wind speed assumed for each release trial was determined by averaging four wind observations at 6 m elevation near

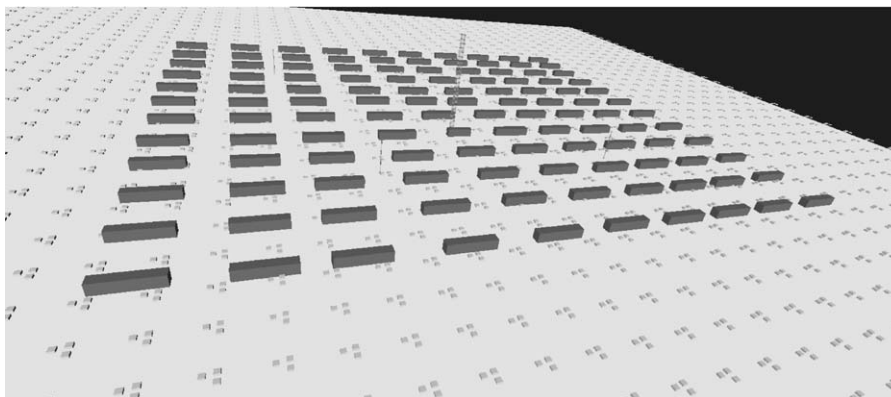


Fig. 1. Locations of 120 obstacles in MUST experiment (described by Biltoft, 2001). This plot was generated by FLACS. The obstacles are 2.54 m high. The numerous groups of three smaller obstacles are intended to represent sagebrush and other bushes on the desert floor. Some towers are shown as vertical lines. The tracer gas was released from various locations between the first and third rows on the upwind (foreground) edge of the array. The four monitoring “arcs” were located between rows 3 and 4, 5 and 6, 7 and 8, and 9 and 10. Downwind distances of the arcs varied with release location but averaged about 25, 60, 95, and 120 m.

Table 1

Performance measures for the 37 trials in the MUST obstacle array, where maximum observed and predicted concentrations on four monitoring arcs are compared

	Median over 4 arcs	Arc 1 (25 m)	Arc 2 (60 m)	Arc 3 (95 m)	Arc 4 (120 m)
Max $C_o$		99.5	35.7	17.2	10.1
Max $C_p$		47.2	13.9	7.73	10.0
Max $C_o$ /Max $C_p$	2.15	2.08	2.56	2.22	1.01
Mean $C_o$		25.5	8.9	5.5	4.2
Mean $C_p$		14.6	5.3	3.0	3.7
FB	0.53	0.55	0.51	0.60	0.45
NMSE	1.64	2.03	1.85	1.44	1.24
MG	1.57	1.44	1.43	1.72	1.70
VG	1.69	1.71	1.44	1.67	2.65
FAC2	0.64	0.68	0.60	0.78	0.59

the corners of the obstacle array. Average wind speed was 3 m/s and the wind direction generally blew from the foreground to the background of the array in Fig. 1. The release locations were altered slightly from trial to trial, but were always near the first three rows of obstacles (near the foreground of Fig. 1). There were four sets of downwind monitoring arrays (at downwind distances of about 25, 60, 95, and 120 m), and the maximum observed and predicted concentrations on each array were compared.

Table 1 summarizes the FLACS model performance for its predictions of maximum concentrations on each arc for the MUST obstacle experiments. The overview in Table 1 suggests that there is an approximate factor of two under-prediction for Max C and about a 36% under-prediction on average. The relative scatter is about 1.5 times the mean. 64% of the predictions are within a factor of two of the observations. These

numbers are within the range of acceptable model performance. There was little trend in model performance with downwind distance.

#### 4.2. Kit fox field experiment

The Kit Fox field experiment took place at the Nevada Test Site, where two types of flat “billboard-shaped” obstacle arrays were used—the larger ERP array (with height 2.4 m) and the smaller URA array (with height 0.2 m). Fig. 2 shows the arrangement of the ERP and URA obstacles as simulated by FLACS. The experiments and some analyses of the data, including comparisons with the HEGADAS dense gas model, are described by Hanna and Chang (2001). All experiments took place in the evening near sundown, and the average wind speed was about 2.5 m/s. There was a total of 52 experiments, but these have been split into four sets for

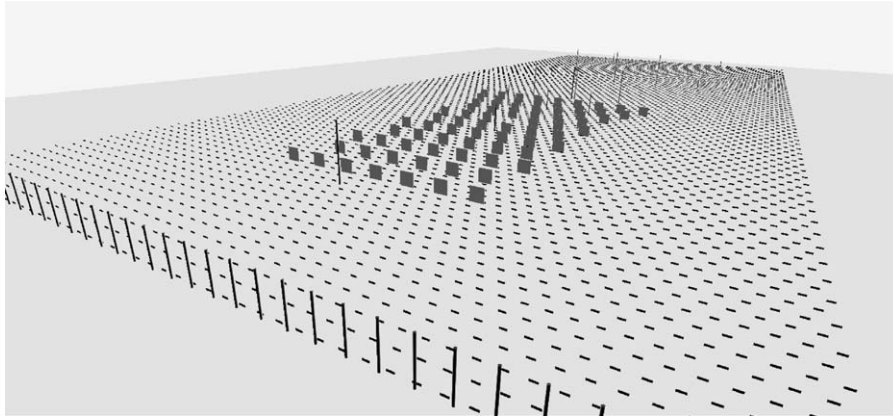


Fig. 2. Locations of obstacles in Kit Fox experiment (described by Hanna and Chang, 2001). This plot was generated by FLACS. The inner array of larger (2.4 m high) obstacles is called the ERP array. The large rectangular area is covered by 0.2 m high obstacles called the URA array. A line of Counihan turbulence generators is seen on the upwind (left) edge. Meteorological towers and vertical sampling towers are seen as vertical lines. The release was from a 1.5 m  $\times$  1.5 m area source near the middle of the ERP array.

Table 2

Performance measures for Kit Fox field experiment, where maximum observed and predicted concentrations on monitoring arcs (at 25, 50, 100, and 225 m) are compared, and statistics represent medians over the four arcs

Data subset	ERP Plumes	ERP Puffs	URA Plumes	URA Puffs	Overall
N	6	13	12	21	52
Mean wind speed	1.7 m/s	2.1 m/s	2.9 m/s	3.0 m/s	2.5 m/s
Max $C_o$ /Max $C_p$	0.64	0.88	1.81	1.51	1.22
FB	0.03	0.07	0.37	0.09	0.08
NMSE	0.30	0.15	0.22	0.12	0.18
MG	1.05	1.19	1.41	1.06	1.12
VG	1.17	1.36	1.22	1.14	1.20
FAC2	1.00	0.90	0.96	0.92	0.94

Results are given for the overall comparisons for the 52 trials and for four subsets of the data for plume versus puff releases and for ERP (2.4 m high) obstacles and for URA (0.2 m high) obstacles.

our statistical analysis: 6 ERP trials with “plume” releases (duration of 120 s or greater), 13 ERP trials with “puff” releases (duration of 20 or 25 s), 12 URA trials with “plume” releases, and 21 URA trials with “puff” releases.  $CO_2$  gas was released at ground level from a 1.5 m  $\times$  1.5 m square opening near the middle of the obstacle array. In all experiments, the maximum observed and predicted concentrations on each of the four monitoring arcs (at 25, 50, 100, and 225 m) were evaluated.

Table 2 presents the Kit Fox performance measures separately for the four sets of release types and obstacle types. The Kit Fox field experiment can be considered to represent four independent sets of trials. The FLACS model performance is seen to be fairly good for each of the four sets of trials, with a relative mean bias less than  $\pm 20\%$  and a relative scatter of 50% or less. Over 90% of the model predictions are within a factor of two of observations. A slight trend is seen for the maximum

concentration for the sets of trials, with a 30 or 40% over-prediction for the ERP (2.4 m high) array and a 30 or 40% under-prediction for the URA (0.2 m high) array. There is little trend with wind speed, stability, or downwind distance.

#### 4.3. Prairie grass field experiment

The Prairie Grass field experiment has become the standard database used for evaluation of models for continuous plume releases near the ground over flat terrain (ASTM, 2000). The site consisted of an agricultural field where the grass had been cut and was short dry stubble at the time of the experiments. The fundamental data report is by Barad (1958), although there are hundreds of published papers describing various methods of analysis of the data. A continuous trace amount of neutrally buoyant gas was released from a small tube at a height of 0.46 m. There were 43 trials in

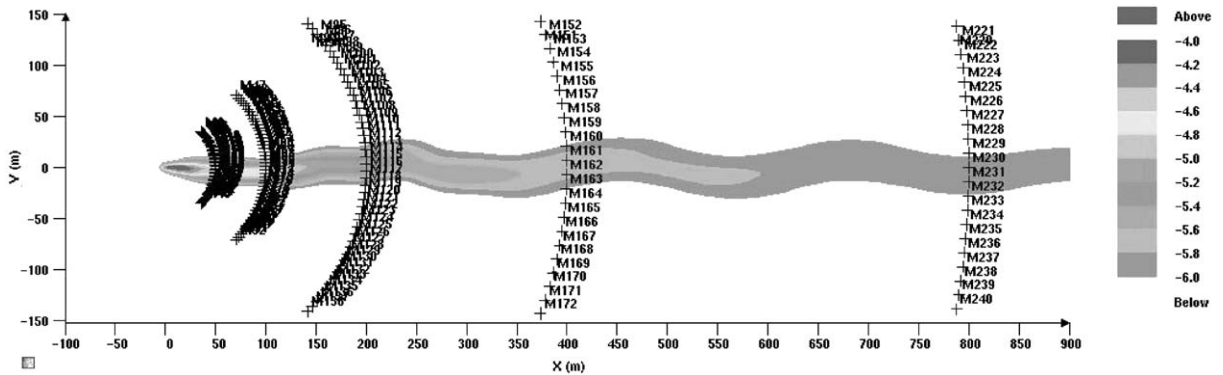


Fig. 3. Locations of five arcs ( $x=50, 100, 200, 400,$  and  $800$  m) in the Prairie Grass experiment (described by Barad, 1958) and an example of a FLACS prediction (PG test 21, Stability D,  $6$  m/s). Predicted concentration is shown in a logarithmic scale where concentrations range from ppm ( $-6$ ) to  $100$  ppm ( $-4$ ).

Table 3

Performance measures for Prairie Grass field experiment, where maximum observed and predicted concentrations on five monitoring arcs ( $50, 100, 200, 400,$  and  $800$  m) are compared. There are 43 trials

	Median over five arcs	Arc 1 (50 m)	Arc 2 (100 m)	Arc 3 (200 m)	Arc 4 (400 m)	Arc 5 (800 m)
Max $C_o$		339	195	111	49.9	37.0
Max $C_p$		259	174	93.7	65.7	30.2
Max $C_o$ /Max $C_p$	1.18	1.31	1.12	1.18	0.76	1.22
Mean $C_o$		122.1	47.8	20.4	8.10	3.69
Mean $C_p$		65.7	28.7	17.1	8.19	4.11
FB	0.18	0.60	0.44	0.18	-0.01	-0.11
NMSE	0.43	0.543	0.426	0.236	0.437	0.348
MG	1.53	2.63	2.20	1.53	0.84	0.35
VG	2.75	4.31	2.75	1.61	1.94	16.9
FAC2	0.49	0.49	0.48	0.62	0.67	0.47

a variety of stability conditions and with an average wind speed of  $5$  m/s. In all experiments, the maximum observed and predicted concentrations were evaluated at a height of  $1.5$  m on each of the five monitoring arcs (at  $50, 100, 200, 400,$  and  $800$  m). Fig. 3 shows the locations of the samplers on the monitoring arcs, and gives an example of a FLACS simulation.

Table 3 contains a summary of the performance measures for the Prairie Grass experiment. Emphasis is on maximum concentrations at given downwind distance arcs. FLACS shows a slight ( $20\%$ ) average relative under-prediction. The relative scatter averages about  $70\%$  to a factor of two. Although it cannot be seen in Table 1, a break-down by stability class would reveal an over-prediction tendency at the more distant arcs ( $400$  and  $800$  m) during unstable (daytime) conditions, as found for most other models. It is thought (see Weil et al., 1992) that convective eddies were “lifting” the observed plume off the ground during the most unstable trials. However, the performance statistics for stable conditions were satisfactory at the  $400$  and  $800$  m arcs.

#### 4.4. EMU L-shaped building wind tunnel experiment

The evaluation of model uncertainty (EMU) study involved a comprehensive evaluation of models in a European Commission—sponsored study described by Hall (1997). Several research laboratories participated in the wind tunnel experiments, the model runs, and the evaluations. The current evaluation used only one of the EMU scenarios—a single L-shaped building (see Fig. 4) located on a flat surface. Neutral ambient conditions were assumed and a continuous release of neutrally buoyant gas took place from a “courtyard” door. Detailed wind tunnel observations were made of flow and dispersion. In the current paper, the concentration predictions at a few locations are compared with the wind tunnel observations. Also, the approximate dimensions of the predicted recirculation zones are compared with observations.

Predicted concentrations at a few cross-wind locations on the cross-section at a distance  $H$  downwind of the lee edge of the L-shaped building were compared with the

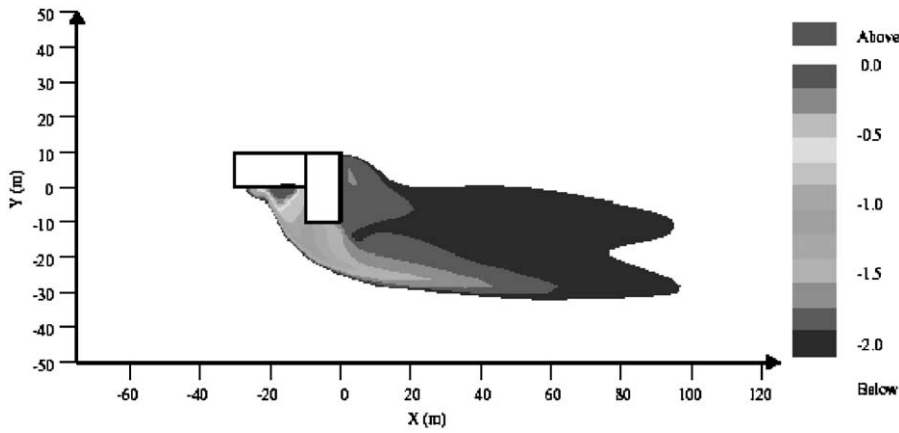


Fig. 4. View from above of EMU L-shaped building, showing coordinate system and example of predicted FLACS concentration distribution. Note that the building height,  $H$ , equals 10 m. The tracer gas release was from a door shown as a thick line at  $y=0.0$  m and between about  $x=-18$  m and  $x=-14$  m.

Table 4  
Comparisons of FLACS predicted concentrations versus observed concentrations (from wind tunnel) for EMU L-shaped building

$y/H$	-2	-2	-2	-1.5	-1.5	-1.5	-1.0	-1.0	-1.0
	$C_o$	$C_p$	$C_o/C_p$	$C_o$	$C_p$	$C_o/C_p$	$C_o$	$C_p$	$C_o/C_p$
$z/H = .16$	0.84	0.60	1.40	1.1	0.36	3.06	0.88	0.36	2.44
$z/H = .37$	0.62	0.34	1.82	0.95	0.30	3.17	0.83	0.32	2.59
$z/H = .67$	0.27	0.13	2.08	0.50	0.22	2.27	0.63	0.29	2.17
$z/H = 1.02$	0.05	0.034	1.47	0.25	0.079	3.16	0.44	0.23	1.91
$z/H = 1.47$	0.01	0.010	1.00	0.03	0.021	1.43	0.13	0.06	2.17
$z/H = 1.99$	0.005	0.004	1.25	0.01	0.009	1.11	0.017	0.026	0.65
Median			1.43			2.72			2.17
FAC2	0.83			0.33			0.33		
$y/H$	-0.5	-0.5	-0.5	0.0	0.0	0.0	0.5	0.5	0.5
	$C_o$	$C_p$	$C_o/C_p$	$C_o$	$C_p$	$C_o/C_p$	$C_o$	$C_p$	$C_o/C_p$
$z/H = .16$	0.63	0.38	1.66	0.3	0.45	0.67	0.18	0.36	0.50
$z/H = .37$	0.63	0.38	1.66	0.5	0.53	0.94	0.32	0.53	0.60
$z/H = .67$	0.63	0.36	1.75	0.6	0.60	1.00	0.48	0.79	0.61
$z/H = 1.02$	0.58	0.34	1.71	0.7	0.75	0.93	0.62	1.05	0.59
$z/H = 1.47$	0.45	0.24	1.88	0.6	0.71	0.85	0.36	0.63	0.57
$z/H = 1.99$	0.05	0.08	0.63	0.1	0.12	0.83	0.067	0.11	0.61
Median			1.68			0.89			0.60
FAC2	1.00			1.00			1.00		

At  $x/H = 1.0$  (i.e., one building height downwind of the lee of the building) for six different heights ( $z/H = 0.16, 0.37, 0.67, 1.02, 1.47,$  and  $1.96$ ), and for six different lateral positions ( $y/H = -2, -1.5, -1.0, -0.5, 0.0,$  and  $0.5$ ).  $y = 0.0$  along the center of the lee building wall and  $y$  is positive towards the longer side of the building. These data were used to generate the scatter plot in Fig. 6.

wind tunnel observations, and the results are given in Table 4. The “steady-state” solution is given, without accounting for meandering fluctuations, since a wind tunnel does not tend to have as many meandering fluctuations as the real atmosphere. Concentrations at 36 locations are compared in the table (at  $y/H = -2.0, -1.5, -1.0, -0.5, 0.0,$  and  $0.5$ ; and at  $z/H = 0.16, 0.37, 0.67, 1.02, 1.47,$  and  $1.99$ ). In general 72% of the predictions are within a factor of two of the observations

and the cross-wind and vertical profiles were well-simulated. The median value of  $C_o/C_p$  is 1.55, implying about a 35% under-prediction. Fig. 5 shows the scatter plot of the data in Table 4, again showing the good agreement but the slight under-prediction tendency. In addition, based on the systematic wind vector variations in Fig. 6, the dimensions of the predicted re-circulating cavities were in agreement ( $\pm 50\%$ ) with known similarity relations based on wind-tunnel observations

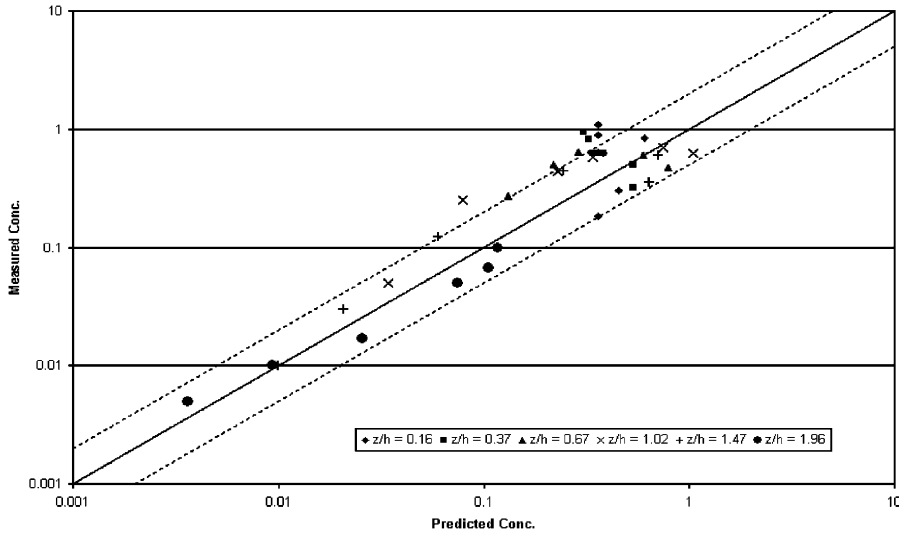


Fig. 5. Scatter plot of FLACS predicted concentrations versus observed concentrations for EMU L-shaped building, at  $x/H = 1.0$  (i.e., one building height,  $H$ , downwind of the lee of the building) for six different heights ( $z/H = 0.16, 0.37, 0.67, 1.02, 1.47$ , and  $1.96$ , and for six different lateral positions ( $y/H = -2, -1.5, -1.0, -0.5, 0.0$ , and  $0.5$ ).  $y = 0.0$  along the center of the lee building wall and  $y$  is positive towards the longer side of the building.

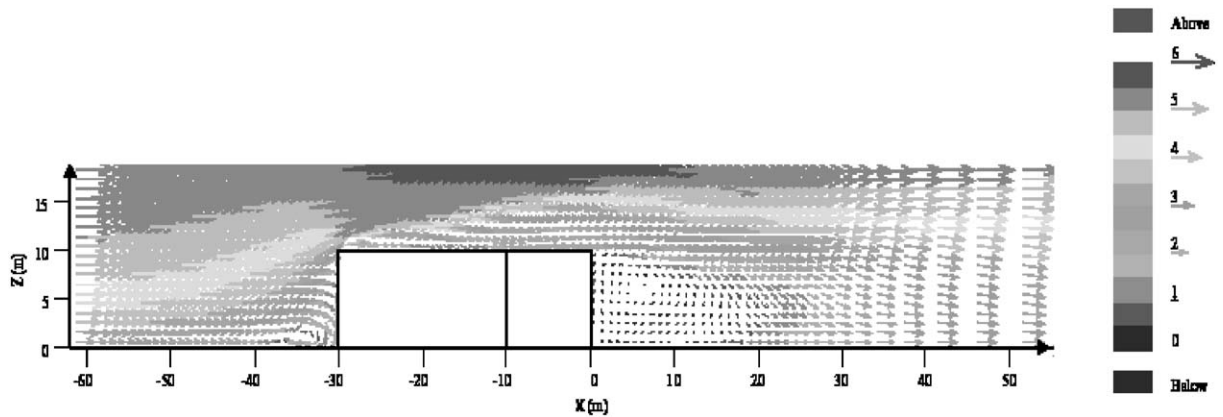


Fig. 6. Cross-section in  $x$  and  $z$  of wind vectors predicted by FLACS for EMU L-shaped building.

(Hanna et al., 1982). The wind tunnel observations and empirical formulas in Hanna et al. (1982) suggest that the length of the re-circulating wake or cavity in the lee of the L-shaped building is about 1.0 to 1.5 times  $H$ , whereas the FLACS prediction in Fig. 6 for this length is about 1.5–2.0.

4.5. Summary of evaluation results

Table 5 contains a summary of the performance measures for the FLACS model applied to the MUST, Kit Fox, and Prairie Grass field experiment data. The medians and ranges of the statistics were determined from the 25 sets of ranked numbers (4 arcs for MUST, 4 subsets of trials times 4 arcs = 16 arcs for Kit Fox, and 5

arcs for Prairie Grass). The medians for the max  $C_o$ /max  $C_p$ , FB, and MG suggest a general under-prediction tendency of about 20%. The medians for NMSE and VG suggest a relative scatter of about 50%. About 86% of the predictions are within a factor of two of the observations. These results are all well within the range of acceptable model performance. The table also contains two estimates of the range of the 25 ranked numbers. First the total range is given, and then the range for 50% of the data (the range from the 7th to the 18th ranked values) is given. The 50% range is fairly tight for field data, suggesting only about a  $\pm 20\%$  range in the relative mean bias and the relative scatter.

In addition, FLACS was evaluated with the wind tunnel observations of the EMU L-shaped building,

Table 5

Median performance measures and “total range” and “inner 50% range” or range for 50% of data closest to median over Kit Fox, MUST, and Prairie Grass field experiments for FLACS CFD model

	Median	Total range	Inner 50% range
Max $C_o$ /Max $C_p$	1.22	0.56 to 2.56	0.94 to 1.86
FB	0.18	−0.32 to 0.60	0.03 to 0.44
NMSE	0.29	0.07 to 2.03	0.17 to 0.44
MG	1.32	0.35 to 2.63	1.06 to 1.47
VG	1.28	1.07 to 17.9	1.15 to 1.94
FAC2	0.86	0.47 to 1.00	0.67 to 1.00

showing that about 72% of the predictions are within a factor of two of the observations, and that there is a tendency towards under-prediction by about 35%. The predicted dimensions of the re-circulating cavity behind the building are within 50% of the known size of the cavity.

For the MUST and Prairie Grass field experiments, where the source aperture was relatively small (on the order of 1 cm), the FLACS simulation guidelines would require a much better grid resolution near the source than has been applied in the calculations reported in this paper. However, this increased resolution would have required very much longer simulation times on the PCs. The lack of local grid refinement may have been partly responsible for the slight under prediction tendency reported above. To improve the results, methods with local grid refinement near the source or analytical models for the initial plume development could be considered.

## 5. Conclusions

This paper describes the evaluation of the FLACS air dispersion model. The model was evaluated using four data sets and using quantitative performance measures, including the fractional bias (FB), the geometric mean (MG), the normalized mean square error (NMSE), the geometric variance (VG), and the fraction of data where predictions are within a factor of two of observations (FAC2). The performance measures reported in many model evaluation exercises with many sets of field data were reviewed in order to determine the characteristics of a “good” or “acceptable model. It was concluded that, for research-grade field experiments, a “good” model would be expected to have at least 50% of the predictions within a factor of two of the observations, a relative mean bias within  $\pm 30\%$ , and a relative scatter of about a factor of two or three.

The performance of the FLACS model is well within these performance criteria, since about 86% of the

predictions are within a factor of two of the observations, the relative mean bias is about 20% from the perspective of FB and about 30% from the perspective of MG, and the relative scatter is about 50 or 60%. The FLACS performance measures are consistent across the three field experiments and the one wind tunnel experiment, and there are minimal trends with distance.

The large numbers of independent atmospheric dispersion experimental trials that have been evaluated with the FLACS CFD model are much more extensive than previously reported in the literature for any CFD model. The authors are already in contact with other CFD modelers who have requested the data sets and have their own evaluation exercises underway. It is hoped that the major contribution of this paper can be to establish an evaluation methodology that will allow comparative CFD model evaluations and spur collaborative efforts to improve model formulations.

## Acknowledgements

This research was supported by the DuPont Company. Steven Hanna’s research on model evaluation methods was also supported by the Defense Threat Reduction Agency (DTRA), the Department of Energy, and the Department of Homeland Security. The authors appreciate the cooperation of Richard Fry of DTRA in providing access to the MUST data.

## References

- Arntzen, B.A., 1998. Modelling of turbulence and combustion for simulation of gas explosions in complex geometries, PhD Thesis, NTNU, Trondheim, Norway, ISBN 82-471-0358-3.
- Arya, S.P., 2001. Introduction to Micrometeorology, Second Edition. ISBN 0-12-059354-8, Academic Press, London, 420 pp.
- ASTM, 2000. Standard guide for statistical evaluation of atmospheric dispersion model performance. American Society for Testing and Materials, Designation D 6589-00. ASTM, 100 Barr Harbor Drive, West Conshohocken, PA 19428–2959.
- Barad, M.L.(Ed.), 1958. Project Prairie Grass. A field program in diffusion. Geophys. Res. Paper No. 59, Vols. I and II, AFCRF-TR-58-235, Air Force Cambridge research Center, Bedford, MA.
- Biltoft, C.A., 2001. Customer Report for Mock Urban Setting Test (MUST). DPG Doc. No. WDTC-FR-01-121, West Desert Test Center, U.S. Army Dugway Proving Ground, Dugway, UT 84022-5000.
- Brown, M., Leach, M., Calhoun, R., Smith, S., Stevens, D., Reisner, R., Lee, R., Chan, S., deCroix, D., 2001. Multiscale modeling of air flow in Salt Lake City and the surrounding region. Proceedings, ASCE Structures Congress 2001,

- Washington, DC. Report LA-UR-01-509, Los Alamos National Lab, Los Alamos, NM 87545
- Chang, J.C., Hanna, S.R., 2004. Air quality model performance evaluation. *Meteorol. Atmos. Phys.* to appear in.
- Gjesdal, T., 2000. Local grid refinement for improved description of leaks in industrial gas safety analysis. *Compute Visual Sci.* 3, 25–32.
- Hall, R.C.(Ed.), 1997. Evaluation of Model Uncertainty (EMU)—CFD modelling of near-field atmospheric dispersion. Project EMU Final Report to the European Commission (Data CD also available with report)7. WS Atkins Doc No. WSA/AM5017/R7, WS Atkins, Woodcote Grove, Ashley Road, Epsom, Surrey KT18 5BW, UK.
- Han, J., Arya, S.P., Shen, S., Lin, Y.-L., 2000. An estimation of turbulent kinetic energy and energy dissipation rate based on atmospheric boundary layer similarity theory. NASA/CR-2000-210298, North Carolina State University, Raleigh, North Carolina.
- Hanna, S.R., Chang, J.C., 2001. Use of the Kit Fox field data to analyze dense gas modeling issues. *Atmos. Environ.* 35, 2231–2242.
- Hanna, S.R., Chang, J.C., Strimaitis, D.G., 1993. Hazardous gas model evaluation with field observations. *Atmos. Environ.* 27A, 2265–2285.
- Hanna, S.R., Tehranian, S., Carissimo, B., Macdonald, R.W., Lohner, R., 2002. Comparisons of model simulations with observations of mean flow and turbulence within simple obstacle arrays. *Atmos. Environ.* 36, 5067–5079.
- Hansen, O.R., Talberg, O., Bakke, J.R., 1999a. CFD-based methodology for quantitative gas explosion risk assessment in congested process areas: examples and validation status. Proceedings, AIChE/CCPS International Conference and Workshop on Modeling the Consequences of Accidental Releases of Hazardous Materials, September 28–October 1, 1999, San Francisco, USA, ISBN 0-8169-0781-1, pp. 457–477.
- Hansen, O.R., Storvik, I., van Wingerden, K., 1999b. Validation of CFD-models for gas explosions, where FLACS is used as example; model description and experiences and recommendations for model evaluation. Proceedings European Meeting on Chemical Industry and Environment III, Krakow, Poland, available at the Department of Environmental Systems Engineering, Faculty of Process and Environmental Engineering, Technical University of Lodz, ul. Wolczanska 175, 90-924 Lodz, Poland, pp. 365–382.
- Hansen, O.R., Renoult, J., Bakke, J.R., 2001. Explosion risk assessment: how the results vary with the approach chosen. Fall Symposium Proceedings, Mary Kay O' Connor Process Safety Centre, Dept. of Chemical Engineering, Texas A&M University, 3122 TAMU, College Station, TX 77843-3122, pp. 395–410.
- Hansen, O.R., 2003. Water deluge and influence on dispersion. FABIG Newsletter Article R485, FABIG, The Steel Construction Institute, Silwood Park, Ascot, Berkshire, SL5 7QN, UK.
- Harlow, F.H., Nakayama, P.I., 1967. Turbulence Transport Equations. *Phys. Fluids* 10, 2323–2332.
- Hjertager, B.H., 1985. Computer simulation of turbulent reactive gas dynamics. *J. Model. Identification Control* 5, 211–236.
- Hjertager, B.H., 1986. Three-dimensional modeling of flow, heat transfer, and combustion. *Handbook of Heat and Mass Transfer*. Gulf Publishing Company, P.O. Box 2608, Houston, Texas 770011, pp. 304–350 Chapter 41
- Hjertager, B.H., Bjørkhaug, M., Fuhre, K., 1988a. Gas explosion experiments in 1:33 scale and 1:5 scale; offshore separator and compressor modules using stoichiometric homogeneous fuel–air clouds. *J. Loss. Prev. Process Ind.* 1, 197–205.
- Hjertager, B.H., Bjørkhaug, M., Fuhre, K., 1988b. Explosion propagation of non-homogeneous methane-air clouds inside an obstructed 50 m<sup>3</sup> vented vessel. *J. Haz. Mater.* 19, 139–153.
- NORSOK Z-013, 2001. Risk and emergency preparedness analysis, Norsok standard. Available from Standard Norge, Postboks 242, N-1326 Lysaker, Norway.
- Patankar, S.V., 1980. *Numerical Heat Transfer and Fluid Flow*, Hemisphere Pub, ISBN: 0070487405
- Riddle, A., Carruthers, D., Sharpe, A., McHugh, C., Stocker, J., 2004. Comparisons between FLUENT and ADMS for atmospheric dispersion modeling. *Atmos. Environ.* 38, 1029–1038.
- Sklavounos, S., Rigas, F., 2004. Validation of turbulence models in heavy gas dispersion over obstacles. *J. Haz. Mater. A.* 108, 9–20.
- Van Wingerden, K., Hansen, O.R., Foisselon, P., 1999. Predicting blast over pressures caused by vapor cloud explosions in the vicinity of control rooms. *Process Safety Progress* 18, 14–17, Available from American Institute of Chemical Engineers, Center for Chemical Process Safety, 3 Park Ave, New York, N.Y., 10016–5991.
- Weil, J.C., Sykes, R.I., Venkatram, A., 1992. Evaluating air-quality models: review and outlook. *J. Appl. Meteor.* 31, 1121–1145.